Consolidation Mechanisms of Pharmaceutical Solids: A Multi-Compression Cycle Approach

Davar Khossravi[1,2,3] and William T. Morehead[2]

Received December 30, 1996; accepted April 29, 1997

Purpose. The consolidation behavior of various pharmaceutical solids were characterized using compression-cycle profiles. Compression-cycle profiles for both uncompacted powder and formed tablets were obtained. These profiles were used to qualitatively and quantitatively characterize the consolidation mechanism of pharmaceutical solids.

Methods. An Instron Universal Testing apparatus and a specially instrumented die coupled with a computerized data acquisition system were utilized to measure the upper-punch pressure and the corresponding die-wall pressure during the compression cycle.

Results. Compression cycle profiles were obtained for a variety of pharmaceutical materials. Based on these profiles, parameters such as hysteresis areas, loading slopes, and unloading slopes were calculated for the materials studied.

Conclusions. Materials that consolidate by plastic deformation have similar compression cycle profiles for the first and subsequent compression cycles indicating that the plastic deformation process occurs to the same extent on the first as well as subsequent compression cycles. For brittle materials, the brittle fracture process occurs during the first compression cycle. During subsequent cycles the tabletted material does not undergo further yield or failure and primarily undergoes elastic deformation. Low molecular-weight polyethylene glycol is an excellent model material for plastically deforming materials, whereas sucrose or sodium citrate are excellent examples of materials that consolidate by brittle fracture.

KEY WORDS: compression cycle; consolidation mechanism; plastic deformation; brittle fracture; multiple compression; pharmaceutical excipients.

INTRODUCTION

The consolidation of powder into a tablet body can be summarized as the initial packing of the particles and elimination of void spaces in the powder bed. With the subsequent elastic deformation, plastic deformation, and brittle fracture of the particles at their points of contact in the powder bed and the formation of solid mass at higher pressures. The contribution of each consolidation mechanism (plastic deformation or brittle fracture) is present to a varying extent in different materials.

Various techniques have been utilized to determine the extent of these two consolidation mechanisms in pharmaceutical solids. Rate dependency is one such method used by various investigators. Stress relaxation data based on the Maxwell model of visco-elastic behavior indicates (1) virtually no rate dependency for elastic or brittle materials such as Fast-Flo lactose and Dipac sugar. Whereas, for materials that undergo consolidation via plastic mechanisms such as microcrystalline cellulose (Avicel PH101) and modified starch (Sta-Rx 1500) a rate dependency is observed. There is also an increase in the calculated yield pressure with an increase in punch velocity for viscoplastic materials such as maize starch and polymeric materials (2). This is attributed to the reduction of time necessary for the plastic deformation process to occur. For brittle materials such as magnesium and calcium carbonates there is no observed change in the yield pressure with increasing punch velocity.

The ability of the material to relieve stress under pressure has also been used to characterize the consolidation mechanism of materials (3–5). Stress relaxation studies indicate that potassium chloride and sodium chloride undergo consolidation via plastic deformation, whereas potassium citrate and lactose undergo consolidation via brittle fracture. Similarly, the compactibility and compressibility of various compacted powder systems have been characterized using a quasi-static brinell hardness test (6–9). Based on these studies materials such as aspirin, sodium chloride, and potassium bromide undergo consolidation by plastic deformation and materials such as lactose, Emcompress, mannitol, and caffeine undergo consolidation by brittle fracture. Hiestand and Smith (10,11) have also defined three dimensionless tablet indices based on indentation hardness and tensile-strength measurements of different materials. The brittle-fracture index measures the ability or inability of the compact to relieve stress by plastic deformation (12) and is calculated based on comparison of tensile strength of a compact with a hole in its center to a compact without a hole. Based on this index the following materials were ranked from brittle fracture to plastic deformation: methenamine, erythromycin, ibuprofen, sucrose, phenacetin, starch, lactose, and microcrystalline cellulose.

Compression cycle profiles have also been used to characterize the consolidation mechanisms of powders. These profiles characterize the extent of pressure distribution within the powder bed as well as the formed tablet matrix. The initial slope, the terminal slope, and the hysteresis areas of these profiles have been calculated and used to characterize the consolidation mechanism of various materials. For plastic materials such as high-density polyethylene, polyethylene glycol 8000, sodium chloride, corn starch NF, starch 1500, and fully hydrolyzed starch (National 1551) the calculated terminal slopes are approximately one. The terminal slopes are less than one for brittle fracture materials such as glass beads, spray-dried lactose, and dicalcium phosphate (13). The Poisson's ratios calculated from the initial slopes are not particularly useful in characterizing the consolidation behavior of powders. Mathematical relationships indicate that for plastic materials a linear relationship between hysteresis areas and maximally applied upper-punch pressure exist, whereas for brittle materials a quadratic relationship is expected (14). In experimental tests (15) of the mathematical model utilizing plastic materials such as polyvinyl alcohol, polyvinyl chloride, and a copolymer of the two, a linear relationship could not be established, casting doubts as to the validity of the underlying assumptions used to derive the relationship (14). Compression cycle profiles have

[1] Present address: 3M Pharmaceuticals, 3M Center, Bldg 260-4N-12, St. Paul, Minnesota 55144-1000.

[2] DuPont Merck, Pharmaceutical Research and Development, Experimental Station, PO Box 80400, Wilmington, Delaware 19880.

[3] To whom correspondence should be addressed. (e-mail: DKHOSSRAVI@MMM.com)

0724-8741/97/0800-1039$12.50/0

also been used to evaluate the compaction behavior of complex formulation mixtures (16,17). For example, the compression characteristics of acetaminophen has been demonstrated to become more plastic upon granulation with poly vinyl pyrrolidone (16).

In the present study, a novel multi-compression cycle approach is used to qualitatively and quantitatively characterize the consolidation mechanism of various pharmaceutical materials. The consolidation mechanism of the material is characterized based on its compaction characteristics during the first compression cycle when the powder bed is converted into the tablet as well as the subsequent compression cycles, where the tablet is subjected to additional compaction forces. This new approach provides significantly more information which enhances our understanding of the consolidation mechanisms.

EXPERIMENTAL

Materials

The following pharmaceutical excipients were used: Sucrose, NF (Lot # 4010, EM Science), Acetaminophen USP (Lot # 00489930929, Mallinckrodt), Aspirin USP (Lot # 9436220391, Rhone-Poulenc), Avicel Micro-crystalline Cellulose, NF type PH-112 (Lot # 9227, FMC Corporation), Avicel Micro-crystalline Cellulose, NF type PH-102 (Lot # 2332, FMC Corporation), Sodium Citrate Anhydrous powder USP, (Lot # 31231, Penta Manufacturing), Sodium Chloride AR crystals ACS, (Lot # 7581-KJDM, Mallinckrodt), Corn starch NF (Lot # MA4927, National Starch Co.), High Density Polyethylene (Lot # 9002-88-4, Schaetlifix-Pulver 1820/200–400; compaction reference standard kindly provided by Nicholas Lordi). Anhydrous Lactose NF (Lot # MRP509871, Sheffield Products); Lactose Hydrous NF (Lot # MRP422796, Sheffield Products), Sentry Polyox WSRN-750 NF (Polyethylene oxide MW 300,000, Union Carbide), Sentry Polyox WSRN-303 NF (Polyethylene oxide MW 7,000,000, Union Carbide), Carbowax Sentry Polyethylene 1450 Flake NF, FCC grade (Lot # IS622984, Union Carbide), Carbowax Sentry Polyethylene 8000 powder NF, FCC grade (Lot# B652, Union Carbide), Klucel HXFNF (Hydroxypropyl cellulose Lot # 8365, Aqualon), Klucel HXF (Hydroxypropyl cellulose with silicon dioxide, Lot # 8543, Aqualon). Materials were used as received. Environmental conditions were held at 68–72°F and 40–50% RH for all work performed and material storage.

Apparatus

An Instron model 5567 (Canton, MA) with static load cell of 30 KN (Serial # UKO15) along with an instrumented die were used to obtain the compression-cycle profiles. The profiles were obtained by programming the instron using the Merlin software provided (Instron Corporation, Canton, MA). The cross head was programmed to move down at a rate of 5 mm/min until a pressure of 225 MPa was reached. Once this pressure was achieved, the Instron was programmed to move up at the same rate until a force of nearly zero was achieved (0.02 KN). This cycle was immediately repeated four more times for a total of five compression cycles. Based on the distance of cross head traveled versus time data collected, displacement versus time plots were constructed. These plots indicate a true saw-tooth wave pattern with remarkable linearity and no signs of curvature or dwell times at the peak or valley junctions.

The Instrumented Die

The instrumented die was used to measure the amount of pressure transmitted to the die wall. The die was made to accommodate 3/8″ flat-faced tooling and was similar to the design of Rippie and Danielson (18) with two minor modifications. A signal-conditioning amplifier (Model 2210; Vishay Measurements Group, Raleigh, NC) was used to excite the bridge at 2.5 volts. The amplification was set at 3000 times and the filter was set at wide band. The output signal (0 to 10 volts) was fed through a channel on the Instron to the computer. The applied data measured by the load cell of the Instron and the transmitted data were collected simultaneously using the Merlin software. The upper and lower punch along with the instrumented die were held in alignment using a specially fabricated jig which was placed on the base plate of the Instron.

Calibration of the Instrumented Die

The static load cell of the instron was calibrated electronically. The instrumented die was calibrated using silicone rubber (Thermogreen TM LB-2 Septa 13/32″ Supelco, Bellefonte, PA). A two point calibration was used to calibrate the instrumented die through the Instron software. The calibration consisted of zeroing the reading when no radial pressure was applied and then calibrating at 100 MPa when 100 MPa of pressure was applied on the silicon rubber. The 13/32″ septa was slightly larger than the 12/32″ die ensuring a tight fit. An inherent assumption was made that the silicone-based septa utilized would act as a hydraulic fluid and transmit the full applied load uniformly in the radial direction. A manual check of applied pressures versus radial pressures measured using the silicone rubber septa showed excellent linearity in an eight-point calibration curve through the range with a correlation coefficient of 1.000 and a slope 1.001. A similar manual check using Klucel HXFNF (hydroxypropyl cellulose) was linear in the range of 0 to 250 MPa with a slope of 0.941 and a correlation coefficient of 0.999.

Data Collection

The instrumented die wall was lightly coated with magnesium stearate prior to placement of the powder into the die. An appropriate amount of powder necessary to produce a compact of 0.18 inch was used to obtain the compression cycle profiles. This was sufficient to cover the entire sensing element on the instrumented die with thickness of 0.08 inch. The data collected consisted of cross head distance traveled, applied load, and the transmitted load as a function of time. A data point was collected each time the applied pressure changed by 0.14 MPa (0.01 KN). The resolution of the A/D converter was 16 bit.

Data Analysis

The applied punch pressure versus the transmitted die-wall pressure was plotted. The loading portion of the plots is related to the application of pressure on the material until the peak punch pressure is reached. The unloading portion of the plot is related to the lifting of the upper punch pressure from

the material and the subsequent release of the applied pressure. These plots are commonly referred to as pressure cycle profile, compression cycle profile, or compaction profiles (13–15,17,19,20). There is also an hysteresis associated with these profiles and at times they are referred to as hysteresis cycle profiles. A least-squares linear regression was used to determine the slopes of linear portions of the compression cycles for both loading and unloading. The region from 150 to 210 MPa (applied pressure) was used to calculate the loading slopes for all of the materials studied. The region from 160 to 110 MPa (applied pressure) was used for acetaminophen, anhydrous lactose, Avicel PH102, Avicel PH112, Avicel PH302, hydrous lactose, Klucel HXFNF, Klucel HXF, Myplx, sodium chloride, sodium citrate, and sucrose to calculate the unloading slopes. The region from 100 to 30 MPa was used for corn starch, high-density polyethylene, polyox 300K, polox 7 million, polyethylene glycol 1450, polyethylene glycol 8000. The slopes were calculated for the first and the fifth compression-cycle profiles obtained. The correlation coefficient in all cases was greater than 0.999 and was greater than 0.9999 for the majority of the cases. The Hysteresis area for each compression cycle was calculated in Excel® using the trapezoidal rule.

RESULTS AND DISCUSSION

The Multiple Compression Cycle Profiles

The compression-cycle profile for polyethylene glycol 1450, which is a soft, low molecular-weight polymeric material, appears as Figure 1. This material undergoes consolidation by plastic deformation (13). The loading region is linear with a calculated slope of approximately one. This linear region begins at very low punch pressures indicating a material with a very low-yield pressure. The unloading (decompression) portion of the compression profile is also linear with a calculated slope of one. During decompression there is a minor curvature near the peak punch pressure which is associated with the low yield strength of PEG1450. In the lower punch pressure regions there is complete release of die-wall pressure indicating that the material is not capable of sustaining any appreciable die-wall pressure after complete punch liftoff. This is consistent with the low yield strength of the material. The compression profiles for all five compression cycles fall on top of each other, in which, the first cycle represents the compression of the powder into a tablet and the subsequent cycles are further compaction of the formed tablet. The processes which occur during the tabeletting of this material (mainly yield) are similar in the first as well as each subsequent cycle. This indicates that the plastic deformation process is not dependent on the previous processing and/or stressing conditions. A similar profile is obtained for Klucel (hydroxypropyl cellulose) indicating that this material also undergoes consolidation by a plastic deformation process.

For materials that consolidate by brittle fracture, such as sodium citrate and sucrose (7), the compression-cycle profiles are drastically different than the plastically deforming materials (Figure 2). The loading and unloading portions of the compression-cycle profiles have slopes significantly less than one and the first compression-cycle profile is drastically different from the subsequent compression-cycles. During the first compression cycle, the loading portion is related to brittle fracture of the material and the unloading portion corresponds to the elastic deformation of the tablet body. During the subsequent compression cycles, the formed tablet predominately undergoes elastic deformation during both the loading and the unloading stages of compression. It is only at punch pressures of less than 30 MPa that some yield of the formed tablet occurs (as evidenced by an increase in slope for this small region). The fact that the initial compression cycle is significantly different from the subsequent compression cycles is highly indicative that the material undergoes brittle fracture during the first compression cycle and does not undergo further brittle fracture in subsequent compression cycles. In effect, all the fracture that can occur takes place during the first compression. The compact formed during the first compression cycle is capable of withstanding and supporting the subsequent compression cycle loads. Since this indicates that for materials which undergo consolidation by brittle fracture the compression characteristics of the material will be extremely sensitive to previous processing and/or stressing conditions, it is of consequence to the formulation scientist. This may effect the final quality of the tablets formed and possibly result in the performance variability associated with different batches of material.

The compression cycle profile for sodium chloride (Figure 3) exhibits behavior consistent with a plastically deforming material with a high yield strength where work hardening

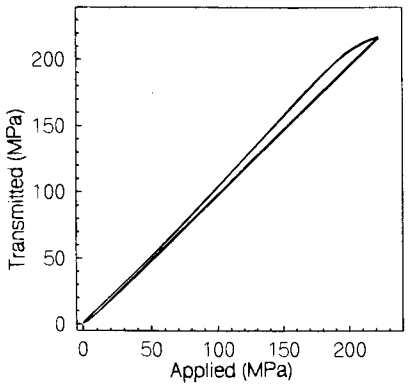

Fig. 1. Multi-compression cycle profile for polyethylene glycol 1450. The profiles for the five consecutive compression cycles are superimposable.

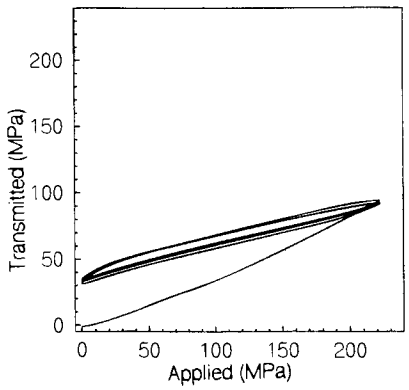

Fig. 2. Multi-compression cycle profile for Sucrose. The first cycle compression starts at the origin. The subsequent compression-cycle profiles are practically superimposable, however, there are very minor changes occurring in subsequent cycles.

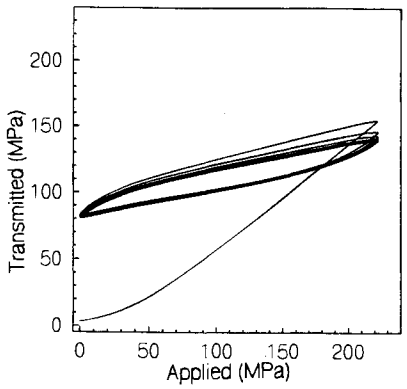

Fig. 3. The multi-compression cycle profile for sodium chloride indicates a plastically deforming material with a high-yield pressure. Subsequent cycles indicate some additional work hardening associated with this material.

occurs. The loading portion of the first compression has a calculated slope of 0.805 and a relatively high yield strength of 60 MPa. The unloading portion is linear with high residual die-wall pressure of 80 MPa indicating a high yield strength for sodium chloride. The second cycle shows a material that yields at a much higher pressure (190 MPa) than the first cycle, but nevertheless does undergo yield, unlike sodium citrate and sucrose. Subsequent cycles are not quite superimposable indicating some additional work hardening occurs during the subsequent compression cycles. Based on the calculated final slope of approximately one for the loading region, Cocals and Lordi (13) have also classified sodium chloride to consolidate by plastic deformation. Brinell hardness measurements on the formed sodium chloride tablets also indicates a plastically deforming material (7). Stress relaxation studies indicate that sodium chloride acts plastically during the compaction process. However, upon formation into tablet is behaves like a brittle material (3,4). This latter observation is more consistent with our results.

Aspirin undergoes consolidation by plastic deformation (Figure 4). It has a moderately low yield strength and does not appear to undergo additional work hardening during the subsequent compression cycles, as is evident by the relative superimposibility of all the compression cycles. The moderately low yield strength and low residual die-wall pressure indicates a material with a low yield pressure which undergoes consolidation by plastic deformation. Leuenberger and coworkers (7) also classify aspirin as a plastically deforming material.

The compression-cycle profiles for the different grades of Avicel that were studied are similar in nature. The compression cycle profile for Avicel 302 (Figure 5) indicates that behavior of this material is intermediate to the two consolidation categories described thus far and perhaps is undergoing consolidation through a combination of brittle fracture and plastic deformation. Hiestand and Smith (21) have made a similar observation for cellulose, lactose, and acetaminophen where mixed regions were observed in which both mechanisms were occurring. Avicel (Microcrystalline cellulose) possesses both crystalline and amorphous regions which is consistent with the brittle fracture and plastic deformation behaviors observed. Reir and Shangraw (22) and Lamberson and Raynor (23) have reported extensive plastic flow during compression of this material which was attributed to numerous slip-planes and dislocations present in the microstructure of Avicel.

Quantitative Analysis of the Compression Cycles

The properties of compression cycle profiles were further analyzed by quantitatively determining the loading and unloading slopes as well as the hysteresis areas associated with the compression cycle profiles. The loading and unloading slopes for the first compression cycle as well as the fifth compression cycle were calculated using least squares linear regression. These values along with their standard deviations appear in Table 1. A bar graph plot of the unloading slopes for the materials studied is presented as Figure 6. A close examination of this plot indicates that materials with unloading slopes of less than 0.4, such as sodium citrate, sucrose, anhydrous lactose, sodium chloride, hydrous lactose, and acetaminophen, fall into one category. Materials which have slopes higher than 0.7, such as polyethylene glycol 8000, high-density polyethylene, polyox 7M, polyox 300K, Myplx, Klucel, and polyethylene glycol 1450 fall into another category. Avicel, corn starch, and aspirin appear to fall in between these two categories indicating that

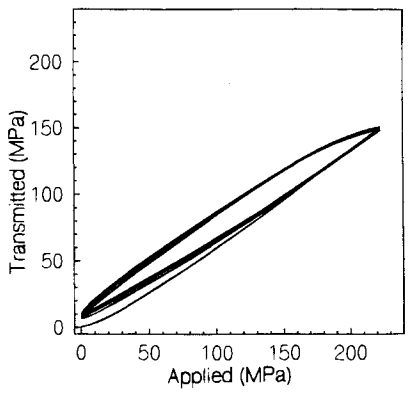

Fig. 4. The multi-compression cycle profile for aspirin indicates that aspirin undergoes consolidation by plastic deformation with a moderate-to-low yield strength. The subsequent compression cycles are fairly superimposable indicating that aspirin does not undergo additional work hardening.

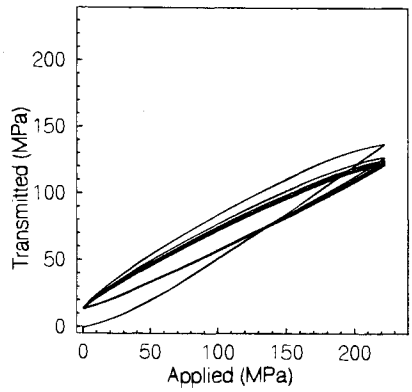

Fig. 5. The multi-compression cycle profile for Avicel 302 (microcrystalline cellulose). This material undergoes consolidation through a combination of brittle fracture and plastic deformation. The subsequent cycles are not quite superimposable.

Table 1. The Calculated Loading Slopes, Unloading Slopes, and Hysteresis Areas for the First and Fifth Compression Cycle Profiles Along with the Calculated Percent Change

	Loading slope (1)	Loading slope (5)	Percent change	Unloading slope (1)	Unloading slope (5)	Percent change	Hysteresis area cycle (1)	Hysteresis area cycle (5)	Percent change
Acetaminophen	0.6094 (0.0003)	0.4035 (0.0002)	66.2	0.3470 (0.0002)	0.32917 (0.00003)	94.9	6290	2720	43.2
Anhydrous Lactose	0.5763 (0.0003)	0.2704 (0.0003)	46.9	0.24455 (0.00006)	0.20804 (0.00018)	85.1	7283	1285	17.6
Aspirin	0.7491 (0.0001)	0.6748 (0.0003)	90.1	0.6596 (0.0008)	0.6165 (0.0007)	93.5	4300	3357	78.1
Avicel PH102	0.69711 (0.00007)	0.5506 (0.0004)	79.0	0.5439 (0.0005)	0.4914 (0.0004)	90.4	4860	2434	50.1
Avicel PH112	0.69557 (0.0003)	0.5634 (0.0004)	81.0	0.5391 (0.0004)	0.4884 (0.0004)	90.6	4914	2555	52.0
Avicel PH302	0.7209 (0.0002)	0.5407 (0.0004)	75.0	0.5206 (0.0004)	0.4715 (0.0004)	90.6	5666	2581	45.6
Corn Starch	0.7909 (0.0001)	0.6922 (0.0002)	87.5	0.7706 (0.0004)	0.6737 (0.0002)	87.4	4942	3383	68.5
HDPE	0.8119 (0.00008)	0.76817 (0.00009)	94.6	0.8855 (0.0007)	0.8278 (0.0006)	93.5	4099	3572	87.1
Hydrous Lactose	0.5640 (0.0003)	0.3577 (0.0002)	63.4	0.3250 (0.0004)	0.3074 (0.0003)	94.6	5707	1490	26.1
Klucel HXFNF	0.8951 (0.0002)	0.8862 (0.0001)	99.0	0.9911 (0.0004)	0.9794 (0.0003)	98.8	1903	1885	99.1
Klucel HXF	0.8970 (0.0002)	0.8871 (0.0002)	98.9	0.9837 (0.0005)	0.9778 (0.0004)	99.4	2180	2034	93.3
Myplx	0.9171 (0.0001)	0.88670 (0.00004)	96.7	0.9600 (0.0006)	0.9514 (0.0006)	99.1	3165	2943	93.0
Sodium Chloride	0.8045 (0.0001)	0.327 (0.002)	40.7	0.25179 (0.00005)	0.19932 (0.00004)	79.2	12725	2795	22.0
Polyox 300K	0.85530 (0.00006)	0.84608 (0.00004)	98.9	0.9462 (0.0005)	0.9273 (0.0003)	98.0	3687	3385	91.8
Polyox 7M	0.85494 (0.00009)	0.84193 (0.00005)	98.5	0.9178 (0.0005)	0.8990 (0.0005)	97.9	3653	3385	92.7
PEG 1450	0.96009 (0.00008)	0.95849 (0.00009)	99.8	1.0633 (0.0002)	1.0590 (0.0002)	99.6	1500	1700	113.3
PEG 8,000	0.8188 (0.0002)	0.7680 (0.0001)	93.8	0.8397 (0.0004)	0.7924 (0.0003)	94.4	4174	2759	66.1
Sodium Citrate	0.42233 (0.00007)	0.2178 (0.0001)	51.6	0.22750 (0.00009)	0.2065 (0.0002)	90.8	4974	808	16.2
Sucrose	0.5112 (0.0004)	0.2384 (0.0002)	46.6	0.2403 (0.0001)	0.2177 (0.0001)	90.6	6340	1108	17.5

Note: The standard deviations appear in parentheses.

both consolidation mechanisms play a role in these materials. The loading slopes for the fifth-compression cycle gives consistent rank ordering of the materials studied.

Based on the compression susceptibility values calculated by Leuenberger and coworkers (7) using the quasi-static brinell hardness method, the materials we have studied can be rank ordered from plastic to brittle as follows: aspirin, Avicel, lactose anhydrous, sodium chloride, and sucrose. Our results indicate a rank ordering of the materials as follows: aspirin, Avicel, lactose hydrous, sodium chloride, lactose anhydrous, and sucrose. The two methods are consistent with the possible exception of lactose. Our study indicates that this difference may be attributed to the hydration state of lactose; which is not clearly mentioned in their study. In light of this fact, the rank ordering of the materials become identical. Leuenberger and coworkers (7) did not include classically plastic materials such as low molecular weight polyethylene glycol, high-density polyethylene, or Klucel (hydroxypropyl cellulose) in their study. Hiestand's brittle fracture index (10) ranks the materials from plastic to brittle as follows: Avicel, spray dried lactose, starch StaRx 1500, and sucrose. Based on the calculated unloading slopes our ranking is: starch, Avicel, lactose, and sucrose. It is apparent that the rank ordering of starch is not consistent which may be attributed to different sources and chemical modifications associated with this material.

Quantitative Analysis of the Hysteresis Areas

The hysteresis areas for the first and fifth compression cycle were calculated using the trapezoidal rule and are reported in Table 1. The hysteresis areas reach a plateau value by the fifth compression cycle, indicating that a quasi-equilibrium state is achieved within the tablet matrix by the fifth cycle. The hysteresis areas for all materials tested except polyethylene

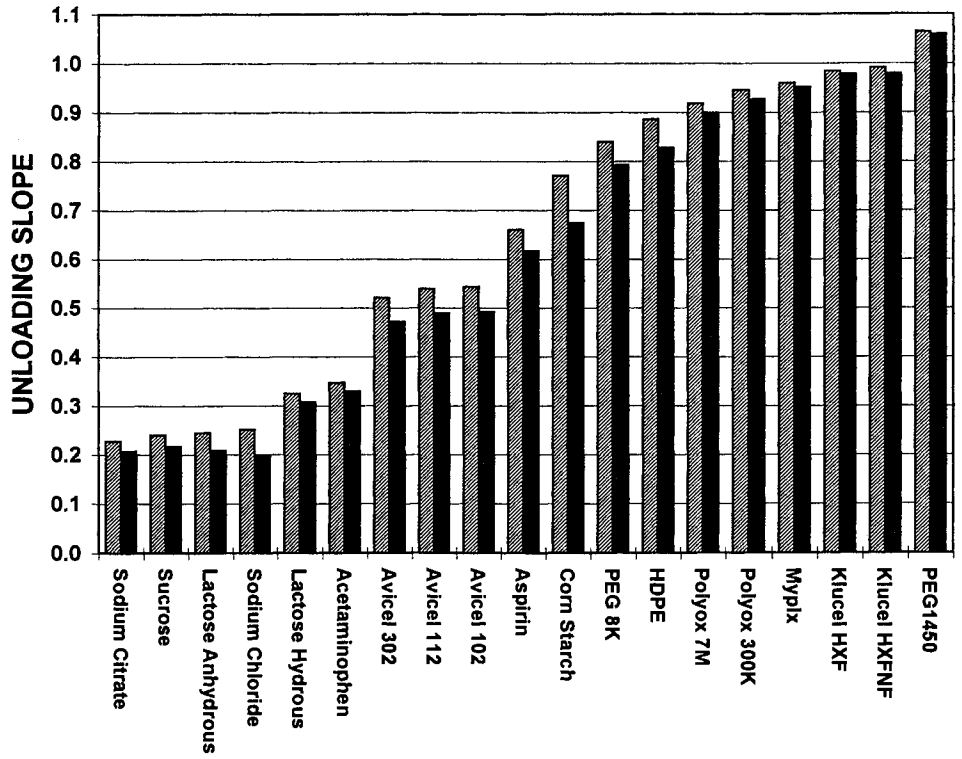

Fig. 6. The unloading slopes calculated for first (hatched) and fifth (solid) compression-cycle profiles for the various materials studied. Materials with unloading slopes of 0.3 or less consolidate via brittle fracture materials, whereas materials with unloading slopes of 0.8 or greater undergo consolidation by plastic deformation.

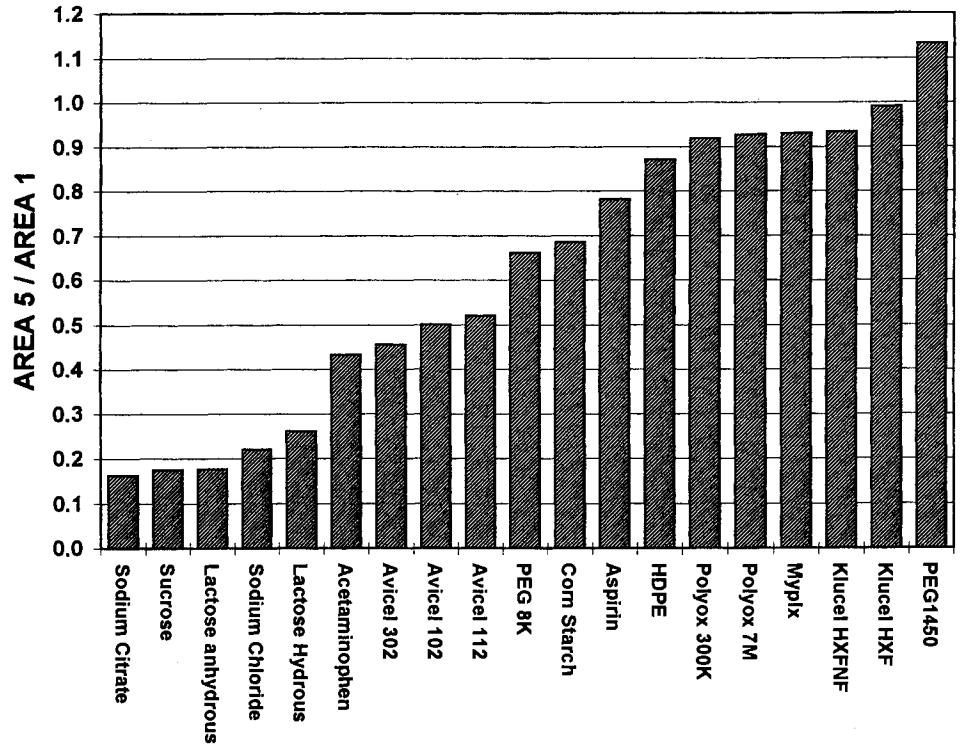

Fig. 7. Hysteresis area ratio (fifth compression cycle hysteresis area to the first compression cycle hysteresis area) for the materials studied.

glycol 1450 is greater for the first compression cycle than for the fifth compression cycle. The ratio of hysteresis area for the fifth compression cycle to be hysteresis area for the first compression cycle is reported in Table 1. This quantity is useful in that it normalizes the areas associated with different materials. For plastically deforming materials the hysteresis ratios approaches one (Figure 7) and in the case of polyethylene glycol 1450 this ratio is actually greater than one. Brittle fracture materials such as sodium citrate, sucrose, anhydrous lactose, and hydrous lactose have hysteresis ratios of less than 0.25. Avicel and corn starch have hysteresis ratios in the range of 0.4 to 0.5 indicating consolidation via both mechanisms.

CONCLUSIONS

1. Examination of initial compression cycles versus subsequent compression cycles is of significant value in evaluating the consolidation mechanisms of various pharmaceutical materials.

2. In general, materials consolidate by plastic deformation or brittle fracture. Some materials, particularly those which have a mixed morphology, such as Avicel, sodium chloride, and corn starch exhibit mixed behavior.

3. In the case of plastic deformation, the first and subsequent compression cycle profiles are superimposable, indicating that the material undergoes the plastic deformation process (yield) in the first as well as each subsequent cycle.

4. In the case of brittle fracture, the first and subsequent compression cycle profiles are not identical, indicating that the material undergoes yield (brittle fracture) during the first cycle only. During the subsequent cycles, the material does not undergo further yield (brittle fracture). The tablet formed behaves elastically in subsequent cycles and is capable of supporting the pressures applied without further yield or failure.

5. Quantitatively, the loading slope on the fifth compression cycle, the unloading slope on the first and fifth compression cycles, and the ratio of hysteresis areas of the fifth compression cycle to the first compression cycle can be utilized to distinguish between consolidation by plastic deformation versus brittle fracture.

6. It is recommended that in future experimentation a low molecular-weight polyethylene glycol should be used as a reference material to characterize the consolidation behavior of plastic materials. Likewise, sucrose or sodium citrate should be used to characterize the consolidation behavior of brittle materials.

ACKNOWLEDGMENTS

Part of this work was presented by DK at the 30th annual Higuchi research meeting. The authors wish to thank Dr. Richard Chang for extremely helpful discussions and suggestions.

REFERENCES

1. T. David and L. L. Augsburger. *J. Pharm. Sci.* **66**:155–159 (1977).
2. R. J. Roberts and R. C. Rowe. *J. Pharm. Pharmacol.* **37**:377–384 (1985).
3. E. T. Cole, J. E. Rees, and J. A. Hersey. *Pharm. Acta. Helv.* **50**:28–32 (1975).
4. J. E. Rees and P. J. Rue. *J. Pharm. Pharmacol.* **30**:601–607 (1978).
5. S. Shlanta and G. Milosovich. *J. Pharm. Sci.* **53**:562–564 (1964).
6. H. Leuenberger and W. Jetzer. *Powder Technol.* **37**:209–218 (1984).
7. W. Jetzer, H. Leuenberger, and H. Sucker. *Pharm. Technol.* **7**:33–39 (1983).
8. H. Leuenberger, E. N. Hiestand, and H. Suker. *Chem.-Ing.-Tech.* **53**:45–47 (1981).
9. H. Leuenberger. *Int. J. Pharm.* **12**:41–47 (1982).
10. E. N. Hiestand and D. P. Smith. *Powder Technol.* **38**:45–59 (1984).
11. E. N. Hiestand and C. Peot. *J. Pharm. Sci.* **63**:605–612 (1974).
12. C. Lipson and R. Juvinall. *Handbook of stress and strength,* Macmillan, New York, 1963.
13. H. G. Cocolas and N. G. Lordi. *Drug Dev. Ind. Pharm.* **19**:2473–2497 (1993).
14. J. T. Carstensen and P. Toure. *Powder Technol.* **26**:199–204 (1980).
15. J. T. Carstensen, J. P. Marty, F. Puisieux, and H. Fessi. *J. Pharm. Sci.* **2**:222–223 (1981).
16. S. Leigh, J. E. Carless, and B. W. Burt. *J. Pharm. Sci.* **7**:888–892 (1967).
17. B. A. Obiorah and E. Shotton. *J. Pharm. Pharmacol.* **28**:629–632 (1976).
18. E. G. Rippie and D. W. Danielson. *J. Pharm. Sci.* **70**:476–482 (1981).
19. W. M. Long. *Powder Metallurgy.* **6**:73–86 (1960).
20. B. A. Obiorah. *Int. J. Pharm.* **1**:249–256 (1978).
21. E. N. Hiestand, and D. P. Smith. *Int. J. of Pharm.* **67**:231–246 (1991).
22. G. E. Reier and R. E. Shangraw. *J. Pharm. Sci.* **55**:510–514 (1966).
23. R. L. Lamberson and G. E. Raynor. *Man. Chem. Aerosol News.* **129**:55–61 (1976).